Citation: Journal of the Optical Society of America A: Optics and Image Science and Vision; Vol. 29, Issue 1, pp. 117-123 (2012)

https://doi.org/10.1364/JOSAA.29.000117

Self-consistent optical constants of sputter-deposited B_4C thin films

Juan I. Larruquert*, Antonio P. Pérez-Marín, Sergio García-Cortés, Luis Rodríguez-de Marcos, José A. Aznárez, José A. Méndez

GOLD-Instituto de Óptica-Consejo Superior de Investigaciones Científicas

Serrano 144, 28006 Madrid, Spain

*Corresponding author: larruquert@io.cfmac.csic.es; fax number: 34 914117651

ABSTRACT

The optical constants of ion-beam-sputtered B_4C films have been measured by ellipsometry in the 190-950 nm range. The set of data has been extended both towards shorter and longer wavelengths with data in the literature, along with inter- and extra-polations, in order to obtain a self-consistent set of data by means of Kramers-Krönig analysis. All data correspond to films that were deposited by sputtering on non-heated substrates, and hence they are expected to be amorphous. B_4C bandgap was calculated as a fitting parameter of Tauc equations for indirect transitions using the present optical constants. A good global accuracy of the data was estimated through the use of various sum-rules. The consistent data set includes the visible to the extreme ultraviolet (EUV); this large spectrum of characterization will enable the design of multilayer coatings that combine a relatively high reflectance in parts of the EUV with a desired performance at a secondary range, such as the visible.

OCIS codes: 120.4530, 160.6000, 310.6860, 260.7200, 230.4170

1. Introduction

Knowledge of the optical constants of materials in a broad spectral range is necessary for demanding applications which require specific performance in such a spectral range. As an example, there are applications for solar physics, astrophysics, lithography or synchrotron radiation that have a primary spectral range in the extreme ultraviolet (EUV; for simplicity here it will refer to wavelengths in the 10-200 nm range; often this range is split into far UV or vacuum UV and EUV) that require a certain performance at a secondary range, such as the visible, near UV or near infrared; for instance a rejection of the visible would be desirable for EUV coatings when solar-blind detectors are not available. In most cases, optical constants of materials, when available, were measured in relatively narrow ranges, and there may be inconsistencies when combining data from different sources.

Boron carbide has been used as an optical coating in the EUV and soft x-rays for various applications. As a single layer coating, it has a moderately high reflectance in the ~50-120 nm range, either as a thin film prepared by ion-beam-sputtering [1,2] or as a bulk prepared by hot pressing [3]. EUV multilayers have also been developed in which sputtered-deposited B_4C films are incorporated into the multilayer both as a constituent [4,5,6,7,8,9] as well as a barrier layer or capping layer [10,11,12] for high-reflectance coatings in the EUV longwards of ~12.5 nm. Sputtered B4C films are also used as constituent materials in soft x-ray multilayers in the region longwards of the B K edge (6.6 nm), which has recently emerged as a wavelength region of interest for next-generation photolithography [13]. Furthermore, single-layer B4C films deposited by magnetron sputtering have recently been implemented as reflective coatings in x-ray free electron laser mirrors, due to their high reflectivity combined with resistance to damage incurred by the high instantaneous radiation dose of the free-electron laser beam [14].

Let us summarize the optical constants of B_4C that are available in the literature. One difficulty with boron carbide is that there is a plethora of materials under this chemical name with compositions in

which the ratio of boron to carbon ranges at least between 2 and 50. As a further complication, B_4C can be prepared by different methods, and the optical properties are expected to depend on the specific preparation method. The references found for the material in the EUV are for the stoichiometry of B_4C, with several works reporting optical constants for thin films, mostly deposited by sputtering on non-heated substrates [2,3,15,16,17,18,19,20]. The few available sets of optical constant data at wavelengths longer than the EUV often refer to various stoichiometries and deposition methods [21,22,23,24], from which only Refs. [22] (only the absorption coefficient) and [24] (both *n* and *k*) involve films with B_4C stoichiometry. Recently, a review on boron carbide material summarizing several physical (including optical) properties has been published [25]. The scant information on the optical constants of B_4C longwards of the EUV may be due to the fact that the material itself does not have attractive optical constants for optics in the visible and close ranges, because it has a relatively large absorption and yet not a high enough reflectance. However, there are applications for EUV coatings that require a certain performance at a secondary range, such as the visible, which turns important the availability of a set of optical constants in a broad spectral range. The purpose of this paper is to provide optical constants of amorphous B_4C films prepared by sputtering on non-heated substrates in a broad spectral range. The paper provides new data measured by ellipsometry in the 190-950 nm and extends this range with literature data and inter- and extra-polations both at shorter and at longer wavelengths, with which a self-consistent set of optical constants is obtained. Section 2 describes the equipment used for sample deposition and characterization. Section 3 displays the obtained optical constants *n*, *k* of B_4C and their extension both to the x-rays and to wavelengths longer than the reststrahlen band. Kramers-Krönig (KK) analysis was used to obtain a self-consistent set of data. Sum-rules are used to estimate the global accuracy of the data.

2. Experimental techniques

B_4C samples were prepared by ion-beam-sputtering (IBS), by impinging energetic ions at ~25° on a target placed facing the substrate. A 96.5-mm diameter, 99.9% purity B_4C target was used. The target was placed in a rotatable target holder that hosts up to 4 targets that are cooled down with water. Ions were produced by means of a 3-cm hollow cathode ion gun working with a hollow cathode neutralizer; this gun and neutralizer contain no filament, which minimizes contamination. Typical deposition conditions were: ion energy of 1,200 eV and a total ion current of 45 mA. Ar was used as a process gas. Thin films were deposited at a rate of ~0.04 nm/s. Film thickness was measured during deposition with a quartz crystal monitor. Si wafers were used as substrates for ellipsometry measurements. A witness glass sample was coated at the same time that the Si substrate; the film thickness of the witness sample was measured a posteriori through Tolansky interferometry, i.e., through multiple-beam interference fringes in a wedge between two highly reflective surfaces [26]. The target-to-substrate distance was 15 cm. The substrate was not intentionally heated or cooled. The sputtering deposition system is placed in a UHV chamber pumped with a cryopump. The base pressure was $7x10^{-8}$ Pa in the sputtering chamber. During deposition, the chamber reached a total pressure of $6x10^{-2}$ Pa.

Ellipsometry measurements were performed with a Ges 5E Sopralab Spectroscopic Ellipsometer. Measurements were performed on samples immediately after taking them out of the vacuum chamber. Ellipsometry measurements started ~5 minutes after first contact with the atmosphere, and they lasted less than 30 minutes. Air exposure was made as short as possible before ellipsometry measurements in order to minimize any oxidation or contamination of the samples prior to measurements, so that intrinsic optical constants of B_4C could be measured.

3. Results and discussion

3.1 DETERMINATION OF OPTICAL CONSTANTS

2 samples of B_4C were prepared, with thicknesses of 37 and 39 nm. Ellipsometry measurements were performed in the 190-950-nm range and the optical constants *n* and *k* were calculated at each measured wavelength. No model for the optical constants of B_4C versus wavelength was assumed in the calculation. Fig. 1 displays the measured ellipsometry parameters $r_p/r_s = \tan(\psi)e^{i\Delta}$ for the 39-nm thick sample and the calculated parameters with the derived optical constants. Fig. 2 displays the obtained optical constants calculated from the ellipsometry measurements, which were averaged over the two samples. The standard deviation, averaged both over the two samples and over the spectrum, amounts 0.012 for *n* and 0.008 for *k*. Likewise we obtain a relative deviation, normalized to n or k, of 0.004 for *n* and 0.015 for *k*. In the calculations, surface roughness was neglected.

The data available in the literature (Refs. [21, 22, 23]) are very different from the present one, the present *k* being much larger; *n* is also very different. This difference is attributed to the very different preparation techniques (Refs. [21, 22, 23]), different stoichiometry (Ref. [23]) and also thicknesses (Refs. [22, 23]; Ref. [21] involves a bulk material) used by the different authors. Here we are focused on samples deposited by sputtering on room-temperature substrates because these are the conditions that we expect for the use of B_4C films in multilayers for optics; film thickness is in the range of the expected ones for multilayers containing B_4C. A hotter substrate during deposition is expected to result in a less-absorbing layer, which would be mostly beneficial for an optical coating; however, for many applications heating the substrate is not possible, since it may be limited by the material resistance (either of substrates or multilayer constituents) and by the possible growth of stress. Regarding various sputtering techniques, we consider that IBS and magnetron sputtering are close techniques that are expected to provide films with similar optical constants; hence below, in the extension of our data to a broader spectrum, we will use data for samples prepared by either

technique, when available. Other than the above, differences in optical constants may arise due to differences in purity and/or on sample ageing. Regarding our samples, they were deposited in UHV with the use of clean pumping and atmosphere exposure was minimized, which suggests that in our samples contamination and oxidation may have been minimized. The present boron carbide *n*, *k* data are the first to extend visible measurements down to the beginning of the EUV at 190 nm, and the first data in the visible for B_4C films deposited on room-temperature substrates by conventional sputtering techniques (versus Ref. [22], where energetic B^+ and C^+ ions impinged on the growing film at much larger energies -100 eV- than in standard sputtering).

In order to generate a set of optical constants that includes at least from the EUV range to the infrared, so that B_4C-based multilayer coatings can be designed for such a broad range, we extended the present range with data from the literature. We gathered *k* data over the spectrum and then we generated *n* with KK analysis; finally, we compared the latter *n* data with our data measured by ellipsometry.

The *k* set gathered here is plotted in Fig. 3. In the extension to the EUV range, we used *k* data of Blumenstock [2] for IBS-B_4C films in the 58.1-175 nm range; these samples were measured after a long contact to atmosphere; a smooth connection between our data and Blumenstock data at 175 nm is referred to in Fig. 3 as interpolation 2. Below 40 nm, the data of Soufli et al. were used [18]; the latter were deposited by DC-magnetron sputtering. In fact, Blumenstock data reached down to 40.6 nm, but the connection with Soufli data was not completely smooth. From the available literature, we found that the data of Monaco et al. [17] measured on samples deposited by RF-magnetron sputtering enabled a good connection to Blumenstock data at 58.1 nm and to Soufli data in the 40-46 nm range; this connection between Soufli data and Blumenstock data using Monaco data is referred to in Fig. 3 as interpolation 1. Soufli data reached 770 eV (1.61 nm); this short-wavelength range

will be expressed in eV. Above 770 eV (not plotted in Fig. 3) we used Henke et al. [27], who obtained a semi-empirical set of data in the 30-10,000-eV range (later extended to 30,000 eV [28]). The density of B_4C amorphous films adopted here was 2.28 g/cm^3 and it was taken from Soufli et al. [14], who measured it for DC magnetron-sputtered B_4C films that were deposited on room-temperature substrates. Henke data were downloaded from the website of the Center for X-Ray Optics (CXRO) at Lawrence Berkeley National Laboratory [29].

The extension to longer wavelengths was more difficult, since we found no data in the literature for close enough samples. As an amorphous semiconductor, B_4C film optical-constant data could be attempted to fit with a Tauc-Lorentz model [30] or other close models. However, that model is not accurate in the range of energies smaller than the bandgap of the material (it will be shown below a calculated bandgap of 0.8 eV) because it assumes no absorption; but of course material absorption will not be zero at energies just below the bandgap, so that Tauc-Lorentz model will not be accurate to describe this range. In view of the above lack of data, we decided to use the optical constants of a close material; B was found as the closest amorphous semiconductor material for which optical constants were available. *k* of B was taken from the self-consistent set of data of Fernández-Perea et al. [31] in the spectral range longer than 950 nm, which used measurements by Morita [32]; B samples in Ref. [32] were films deposited by electron-beam evaporation. To avoid a discontinuity at 950 nm, we smoothly connected our data with those of Ref. [31] at 1400 nm; this connection is referred to as interpolation 3 in Fig. 3. At still longer wavelengths, B_4C is expected to present a reststrahlen band, differently to B; the reason for this is that the reststrahlen band is present when materials have at least partly ionic bonding, as it is the case for B_4C but in principle not for B. We found a reference for the reststrahlen band of B_4C in the paper of Samara et al. [21]; they measured reflectance of polycrystalline B_4C samples that had been grown by hot pressing; they used a KK analysis to obtain the dielectric constant from which we calculated *k*. Their reststrahlen peak was

fitted to a sum of two Lorentz oscillators, which we used in the long wavelength extrapolation and referred to as Reststrahlen in Fig. 3. Regarding the reststrahlen band of a material, its shape is expected to strongly depend on the material being crystalline or amorphous, the band being much sharper and narrower for crystals, as it was reported for SiC [33]. Hence the real reststrahlen band for amorphous B_4C may be wider and shorter than the one used here; unfortunately, we did not find any data on the reststrahlen band for amorphous B_4C in order to perform a more accurate model. To help the eye, the set of *k* data gathered in this full set of *k* data is plotted in Fig. 3 only with lines, whereas symbols refer to various data in the literature.

With this set of *k* in the whole spectrum we could calculate the refractive index *n* of B_4C in the whole spectrum using KK dispersion relations:

$$n(E)-1=\frac{2}{\pi}P\int_0^\infty \frac{E'k(E')}{E'^2-E^2}dE' \qquad (1)$$

where *P* stands for the Cauchy principal value; *E* stands for photon energy. The result is plotted in Fig. 4, along with data in the literature. Since we also had measurements of *n* in the 190-950 nm range, we could check the similarity of both sets of data in this range. *n* data obtained through KK analysis were somewhat smaller than data obtained by ellipsometry in the whole range, averaging a 1.3% difference. The difference was considered small enough so that the present *k* data extended from our ellipsometry measurements along with *n* data obtained by KK analysis is a self-consistent set of optical constants in the whole spectrum that is compatible with our optical constants obtained by ellipsometry. This consistent set of *n*, *k* data was taken as the final result [34].

Let us see the difference in *n*, *k* data with respect to other sources. The difference in δ=1-*n* with respect to the data obtained by Soufli et al. [18] was small away from B K edge at ~188 eV; the relative difference in absolute value averaged 2.4% and 2.8% at energies higher and lower, respectively, than B K edge. At B K edge δ crosses zero; therefore, it is better to use *n* in the

comparison. At B K edge, the difference in *n* with respect to Ref. [18] data averaged 0.03%. The differences with Blumenstock [2] and Monaco [17] are not large in the ranges in which their *k* data were used. There is a somewhat larger deviation with respect to boron in the long wavelengths, which can originate in part from the fact that we are using data of a different material (B versus B_4C) and we also had to adapt the connection, as explained above. Furthermore, the use of the reststrahlen band taken from crystalline B_4C, and not for amorphous material, may be also responsible for part of the deviation.

For crystalline semiconductors, the bandgap is a well-defined parameter, which corresponds to energies of forbidden transitions between the valence and the conduction bands. For amorphous semiconductors, Tauc [35,36] interpreted the presence of some kind of indirect bandgap as representative of optical transitions without momentum conservation between extended states in the valence and conduction bands under the assumption of parabolic bands and constant matrix elements [37]. The bandgap is calculated as a fitting parameter of the absorption coefficient $\alpha=4\pi k/\lambda$ or the imaginary part of the dielectric constant ε_2 [38]. Fig. 5 displays a Tauc plot obtained with the present optical constants by fitting equations:

$$\sqrt{\alpha E} \propto (E - E_G), \tag{2a}$$

$$\sqrt{\varepsilon_2 E^2} \propto (E - E_G), \tag{2b}$$

where E_G is the fitted bandgap energy [38]. From Fig. 5 we obtain E_G=0.78 eV (Eq. 2a) and E_G=0.75 eV (Eq. 2b) by the abscissa intercept of the linear extrapolation. The linear fitting was performed in the 1.6-3.2 eV range, which involves data obtained here. Few data were found in the literature. Ahmad et al. [39] obtained a bandgap of ~0.6 eV for films with B_4C stoichiometry that were deposited by magnetron sputtering with methane-saturated boron carbide target; the function fitted is said to be $\alpha^{1/3}$, although some authors used $(\alpha E)^{1/3}$ [40]; the former function gave us a negative

fitting parameter in this energy range, whereas the latter gave us a bandgap close to 0. Lee et al. [41] measured an indirect bandgap of ~0.8 eV for the present stoichiometry for films prepared by PECVD on substrates at 400ºC; films were determined to be either microcrystalline or amorphous; the authors apparently used also Tauc equations for bandgap calculations. For more crystalline samples, other bandgap values have been obtained ranging between 0.48 eV (Werheit et al. [42], for coarse crystalline and sintered $B_{12}C_3$; they used Tauc equations but had to separate a long-wave tail in some unspecified way) to 2.9-to-4.0 eV (Armstrong et al. [43]; theoretical calculations on $B_{12}C_3$ crystals) and 2.781 eV (Bylander et al. [44]; theoretical calculations on $B_{12}C_3$ crystals); Monaco et al. [24] obtained a gap of 2.41 eV for an amorphous film prepared by PLD on room-temperature substrate, but it was obtained with the equation of direct transitions (an exponent of 2 instead of ½ in Eq. 2; no linear range was found here using an exponent of 2). Furthermore, the bandgap of boron carbides depends on stoichiometry in a way that it increases with the boron-to-carbon ratio. Summarizing, a wide range of bandgaps has been reported for boron carbides and the one obtained here has been calculated with accurate optical data measured on B_4C thin films deposited on room-temperature substrates in UHV conditions after a minimum contact to atmosphere and using Tauc equations for indirect transitions.

3.2 CONSISTENCY OF OPTICAL CONSTANTS

The *f* sum rule relates the number density of electrons to *k* or to other functions; it provides a guidance to evaluate the global accuracy of *k* data. It is useful to define the effective number of electrons per atom $n_{eff}(E)$ contributing to *k* up to given energy *E*:

$$n_{eff}(E) = \frac{4\varepsilon_0 m}{\pi N_{mol} e^2 \hbar^2} \int_0^E E' k(E') dE' \qquad (3)$$

where N_{mol} is the molecular density, *e* is the electron charge, ε_0 is the permittivity of vacuum, *m* is the electron mass, and $\hbar$ is the reduced Planck constant [45]. The *f* sum rule expresses that the high-energy limit of n_{eff} must reach the number of electrons of the atom or molecule involved, which is 26

for B_4C. When the relativistic correction on scattering factors is taken into account, the high-energy limit of Eq. (3) is slightly modified. A modified electron number of 25.98 was adopted here [46]. As mentioned above, the density of B_4C amorphous films to calculate N_{mol} was taken as 2.28 g/cm^3. The high-energy limit that we obtained using Eq. (3) with the consistent data set described in the previous sub-section was 26.80, which is a 3.2% larger than the theoretical value; this deviation can be considered acceptable here taking into account the large number of data sources that were used. From the above number of electrons, 0.88 comes from the spectral range measured by ellipsometry. A larger number of electrons that contribute in this same spectral range is obtained when we replace k in Eq. (3) with ε_2 [47]: the number of electrons coming from the spectral range measured by ellipsometry is then 2.48; with the latter function the total number of electrons using the present optical constants is 26.81. These results suggest that the above deviation in $n_{eff}(\infty)$ originates over the large spectrum gathered here, and not specifically over the ellipsometry range. The deviation may come in part from inconsistencies in the k data used in the energy extrapolations and it probably comes mostly from the EUV-to-short X-rays since these are the ranges with the largest contribution in the integral of Eq. 3.

A useful test to evaluate the accuracy of KK analysis is obtained with the inertial sum rule:

$$\int_0^\infty [n(E)-1]dE = 0, \tag{4}$$

which expresses that the average of the refractive index throughout the spectrum is unity. The following parameter is defined to evaluate how close to zero the integral of Eq. (4) [48] is:

$$\zeta = \frac{\int_0^\infty [n(E)-1]dE}{\int_0^\infty |n(E)-1|dE} \tag{5}$$

Shiles et al. [45] suggested that a good value of ζ should stand within ±0.005. An evaluation parameter $\zeta=9\times10^{-4}$ was obtained with the *n* data calculated in this research. Therefore, the inertial sum rule test is well within the above top value. The main contribution to the integral of Eq. (4) comes from a broad spectral range of ~0.05-6,000 eV, which includes the present ellipsometry range but also many data in a broader range, and has a peak contribution at ~12.7 eV. As with the *f* sum rule, we looked for a specific sum rule that gives more weight to the ellipsometry range. This was obtained by replacing *n* with ε_1 (real part of the dielectric constant) in Eq. (4) [47]; in this case, we must assume a negligible DC material conductivity for the integral to be zero, which seems plausible for amorphous B_4C. With this sum rule an evaluation parameter (immediately generalized from Eq. 5) of $8x10^{-6}$ was obtained, which is even lower than the one obtained above. The main contribution to the integral comes from a similar range than above, but the peak is now at ~8.3 eV, which is closer to the high-energy edge of the present ellipsometry range. This suggests, along with the *f* sum rule, a good consistency of *n* and *k* data set gathered here.

The present self-consistent data set aims at enabling the design of multilayer coatings based on B_4C films with optimized performance in the EUV to near infrared. This task adds to our past efforts to provide similar sets of data on other semiconductors (B [31] and SiC [49]) and insulators (SiO [50]), which will be further addressed with more materials in the near future.

4. Conclusions

The optical constants *n* and *k* of thin IBS B_4C films, which were deposited on room-temperature substrates, have been obtained from ellipsometry measurements in the 190-950 nm spectral range. This data set has been extended to a broad spectrum with literature data, and inter- and extrapolations. With KK analysis we have constructed a consistent set of optical constants; this set will enable the design of coatings optimized over a broad spectral range that includes from the soft x-rays and the EUV, in part of which B_4C mirrors have a moderately large reflectance, to the near infrared. That set is useful for applications for which, in addition to a high reflectance in the EUV, it is required a certain performance at a secondary range, such as the visible. A bandgap of 0.75-0.78 eV was obtained as a fitting parameter of Tauc equations for indirect transitions.

The evaluation of *f* and inertial sum rules shows good consistency of the optical constants gathered for B_4C.

Acknowledgments

This work was supported by the National Programme for Space Research, Subdirección General de Proyectos de Investigación, Ministerio de Ciencia y Tecnología, project number AYA2010-22032. S. García-Cortés, L. Rodríguez-de Marcos, and A. P. Pérez-Marín are thankful to Consejo Superior de Investigaciones Científicas (Spain) for funding under the Programa I3P, partially supported by the European Social Fund. The technical assistance of J. M. Sánchez-Orejuela is acknowledged.

References

1. G. M. Blumenstock and R. A. M. Keski-Kuha, "Ion-beam-deposited boron carbide coatings for the extreme ultraviolet," Appl. Opt. **33**, 5962–5963 (1994).

2. G. M. Blumenstock, R. A. M. Keski-Kuha, and M. L. Ginter, “Extreme ultraviolet optical properties of ion-beam-deposited boron carbide thin films,” in X-Ray and Extreme Ultraviolet Optics, R. B. Hoover and A. B. Walker, eds., Proc. SPIE **2515**, 558–564 (1995).

3. J. I. Larruquert and R. A. M. Keski-Kuha, “Optical properties of hot-pressed B4C in the extreme ultraviolet,” Appl. Opt. **39**, 1537–1540 (2000).

4. J. I. Larruquert, R. A. M. Keski-Kuha, “Multilayer coatings with high reflectance in the EUV spectral region from 50 to 121.6 nm”, Appl. Opt. **38**, 1231-1236 (1999).

5. J. I. Larruquert, R. A. M. Keski-Kuha, “Sub-quarterwave multilayer coatings with high reflectance in the extreme ultraviolet”, Appl. Opt. **41**, 5398-5404 (2002).

6. D. L. Windt, S. Donguy, J. F. Seely, B. Kjornrattanawanich, E. M. Gullikson, C. C. Walton, L. Golub, and E. DeLuca, “EUV multilayers for solar physics”, Proc. SPIE **5168**, 1–11 (2004).

7. F. Delmotte, J. Gautier, M.F. Ravet, F. Bridou, A. Jerome, “Optiques multicouches pour l´extrême UV”, J. Phys. IV France **127**, 69–75 (2005).

8. J. Gautier, F. Delmotte, M. Roulliay, F. Bridou, M.-F. Ravet, A. Jérome, “Study of normal incidence of three-component multilayer mirrors in the range 20-40 nm,” Appl.Opt, **44**, 384-390 (2005).

9. Z. Wang, S. Zhang, W. Wu, J. Zhu, H. Wang, C. Li, Y. Xu, F. Wang, Z. Zhang, L. Chen, H. Zhou, T. Huo, “B4C/Mo/Si high reflectivity multilayer mirror at 30.4 nm,” Chin. Opt. Lett. **4**, 611-613 (2006).

10. S. Bajt, J. B. Alameda, T. W. Barbee, Jr., J. A. Folta, B. Kaufmann, E. A. Spiller, “Improved reflectance and stability of Mo/Si multilayers,” Opt. Eng. **41**, 1797-1804 (2002).

11. S. Braun, H. Mai, M. Moss, R. Scholz, “Microstructure of Mo/Si multilayers with barrier layers”, Proc. SPIE **4782**, 185-195 (2002).

12. T. Böttger, D. C. Meyer, P. Paufler, S. Braun, M. Moss, H. Mai, E. Beyer, “Thermal stability of Mo/Si multilayers with boron carbide interlayers,” Thin Solid Films **444**, 165–173 (2003).

13. Yu. Platonov, J. Rodriguez, M. Kriese, E. Gullikson, T. Harada, T. Watanabe, H. Kinoshita, “Multilayers for next generation EUVL at 6.X nm”, Proc. SPIE **8076**, 80760N (2011).

14. R. Soufli, S. L. Baker, J. C. Robinson, T. J. McCarville, M. J. Pivovaroff, S. P. Hau-Riege, R. Bionta, “Morphology, microstructure, stress and damage properties of thin film coatings for the LCLS x-ray mirrors”, Proc. SPIE **7361**, 73610U (2009).

15. C. Tarrio, R. N. Watts, T. B. Lucatorto, J. M. Slaughter, C. M. Falco, “Optical constants of in situ-deposited films of important extreme-ultraviolet multilayer mirror materials,” Appl. Opt. **37**, 4100–4104 (1998).

16. F. Frassetto, D. Garoli, G. Monaco, P. Nicolosi, M. Pascolini, M.G. Pelizzo, V. Mattarello, A. Patelli, V. Rigato, A. Giglia, S. Nannarone, E. Antonucci, S. Fineschi, M. Romoli, “Space applications of Si/B4C multilayer coatings at extreme ultra-violet region; comparison with standard Mo/Si coatings”, Proc. of SPIE **5901**, 59010L (2005)

17. G. Monaco, D. Garoli, R. Frison, V. Mattarello, P. Nicolosi, M.G. Pelizzo, V. Rigato, L. Armelao, A. Giglia, S. Nannarone, “Optical constants in the EUV Soft x-ray (5 ÷152 nm) spectral range of B4C thin films deposited by different deposition techniques”, Proc. of SPIE **6317**, 631712 (2006).

18. R. Soufli, A. L. Aquila, F. Salmassi, M. Fernández-Perea, E. M. Gullikson, “Optical constants of magnetron-sputtered boron carbide thin films from photoabsorption data in the range 30 to 770 eV”, Appl. Opt. **47**, 4633-4639 (2008).

19. M. Nayak, G. S. Lodha, T. T. Prasad, P. Nageswararao, A. K. Sinha, “Probing porosity at buried interfaces using soft x-ray resonant reflectivity”, J. Appl. Phys. **107**, 023529 (2010).

20. D. Ksenzov, T. Panzner, C. Schlemper, C. Morawe, U. Pietsch, “Optical properties of boron carbide near the boron K edge evaluated by soft-x-ray reflectometry from a Ru=B4C multilayer”, Appl. Opt. **48**, 6684-6691 (2009).

21. G. A. Samara, H. L. Tardy, E. L. Venturini, T. L. Aselage, D. Emin, “ac hopping conductivities, dielectric constants, and reflectivities of boron carbides”, Phys. Rev. B **48**, 1468–1477 (1993)

22. C. Ronning, D. Schwen, S. Eyhusen, U. Vetter, H. Hofsäss, “ Ion beam synthesis of boron carbide thin films”, Surface and Coatings Technology **158 –159**, 382–387 (2002).

23. A. A. Ahmad, N. J. Ianno, P. G. Snyder, D. Welipitiya, D. Byun, and P. A. Dowben, “Optical properties of boron carbide (B5C) thin films fabricated by plasma-enhanced chemical-vapor deposition”, J. Appl. Phys. **79**, 8643-8647 (1996).

24. G. Monaco, D. Garoli, M. Natali, F. Romanato, P. Nicolosi, “Spectroscopic study of beta-SiC prepared via PLD at 1064 nm”, Cryst. Res. Technol. **46**, 784 – 788 (2011).

25. V. Domnich, S. Reynaud, R. A. Haber, M. Chhowalla, “Boron Carbide: Structure, Properties, and Stability under Stress”, Journal of the American Ceramic Society, 2011. doi: 10.1111/j.1551-2916.2011.04865.x

26. S. Tolansky, “Multiple-beam interferometry of surfaces and films”, Oxford University Press, London, 1948.

27. B. L. Henke, P. Lee, T. J. Tanaka, R. L. Shimabukuro, B. K. Fujikawa, “Low-Energy X-Ray Interaction Coefficients: Photoabsorption, Scattering, and Reflection, E = 100-2000 eV, *Z*=1-94”, At. Data Nucl. Data Tables **27**, 1-144 (1982).

28. B.L. Henke, E.M. Gullikson, and J.C. Davis, “X-ray interactions: photoabsorption, scattering, transmission, and reflection at E=50-30000 eV, Z=1-92”, Atomic Data and Nuclear Data Tables **54**, 181-342 (1993).

29. http://henke.lbl.gov/optical_constants/

30. G. E. Jellison, Jr. and F. A. Modine, "Parameterization of the optical functions of amorphous materials in the interband region", Appl. Phys. Lett. **69**, 371-373 (1996).

31. M. Fernández-Perea, J. I. Larruquert, J. A. Aznárez, J. A. Méndez, M. Vidal-Dasilva, E. M. Gullikson, A. Aquila, R. Soufli, and J. L. G. Fierro, "Optical constants of electron-beam evaporated boron films in the 6:8–900 eV photon energy range," J. Opt. Soc. Am. A **24**, 3800–3807 (2007).

32. N. Morita, "Optical constants of boron in visible and near infrared," J. Sci. Res. Inst. **48**, 8–12 (1954).

33. E. A. Fagen, "Optical and electrical properties of amorphous silicon carbide films", in *Amorphous and liquid semiconductors*, volume 1, J. Stuke, W. Brenig, eds., Taylor & Francis, Ltd., London 1974. It contains part of the proceedings of the International Conference on Amorphous and liquid semiconductors held at Garmisch-Partenkirchen, Germany, in 1973.

34. The data are available on request at the following e-mail address: larruquert@io.cfmac.csic.es

35. J. Tauc, R. Grigorovici, A. Vancu, "Optical properties and electronic structure of amorphous germanium", Phys. Stat. Sol. **15**, 627-637 (1966).

36. J. Tauc, "Optical properties and electronic structure of amorphous Ge and Si", Mat. Res. Bull. **3**, 37-46 (1968).

37. M. L. Theye, "Optical properties of a-Ge, a-Si and a-III-V compounds", in *Amorphous and liquid semiconductors*, volume 1, J. Stuke, W. Brenig, eds., Taylor & Francis, Ltd., London 1974. It contains part of the proceedings of the International Conference on Amorphous and liquid semiconductors held at Garmisch-Partenkirchen, Germany, in 1973.

38. O. Stenzel, "The Physics of Thin Film Optical Spectra: An Introduction", Springer-Verlag Berlin Heidelberg 2005, p. 214.

39. A. A. Ahmad, N. J. Ianno, S.-D. Hwang, P.A. Dowben, "Sputter deposition of high resistivity boron carbide", Thin Solid Films **335**, 174-177 (1998).

40. J. Melsheimer and D. Ziegler, “Band gap energy and Urbach tail studies of amorphous, partially crystalline and polycrystalline tin dioxide”, Thin Solid Films, **129**, 35-47 (1985).

41. S. Lee, J. Mazurowski, G. Ramseyer, P. A. Dowben, “Characterization of boron carbide thin films fabricated by plasma enhanced chemical vapor deposition from boranes”, J. Appl. Phys. **72**, 4925-4933 (1992).

42. H. Werheit, H. Binnenbruck, A. Hausen, “Optical properties of boron carbide and comparison with β-rhombohedral boron”, Phys. Stat. Sol. (b) **47**, 153-158 (1971).

43. D. R. Armstrong, J. Bolland, P. G. Perkins, G. Will, A. Kirfel, “The nature of the chemical bonding in boron carbide. IV. Electronic band structure of boron carbide, B13C2, and three models of the structure $B_{12}C_3$”, Acta Cryst. **B39**, 324-329 (1983).

44. D. M. Bylander, L. Kleinman, S. Lee, “Self-consistent calculations of the energy bands and bonding properties of $B_{12}C_3$”, Phys. Rev. B 42, 1394–1403 (1990).

45. E. Shiles, T. Sasaki, M. Inokuti, D. Y. Smith, “Self-consistency and sum-rule tests in the Kramers-Kronig analysis of optical data: applications to aluminium”, Phys. Rev. B **22**, 1612-1628 (1980).

46. Downloaded from the following web of Physical Reference Data, Physics Laboratory at NIST: http://physics.nist.gov/PhysRefData/FFast/html/form.html

47. M. Altarelli, D. L. Dexter, H. M. Nussenzveig, D. Y. Smith, “Superconvergence and Sum Rules for the Optical Constants”, Phys. Rev. B **6**, 4502–4509 (1972).

48. M. Altarelli and D. Y. Smith, “Superconvergence and sum rules for the optical constants: physical meaning, comparison with experiment, and generalization”, Phys. Rev. B **9**, 1290-1298 (1974).

49. J. I. Larruquert, A. P. Pérez-Marín, S. García-Cortés, L. Rodríguez-de Marcos, J. A. Aznárez, J. A. Méndez, “Self-consistent optical constants of SiC thin films”, accepted for publication in Journal of the Optical Society of America A.

50. M. Fernández-Perea, M. Vidal-Dasilva, J. I. Larruquert, J. A. Aznárez, J. A. Méndez, E. Gullikson, A. Aquila, R. Soufli, “Optical constants of evaporation-deposited silicon monoxide films in the 7.1 – 800 eV photon energy range”, J. Appl. Phys. **105**, 113505 (2009).

Figure captions

Fig. 1. (color online) Ellipsometry parameters tanψ and cosΔ, both experimental and fitted, measured at 72^o as a function of wavelength.

Fig. 2. (color online) The optical constants *n* and *k* obtained from ellipsometry measurements as a function of wavelength.

Fig. 3. (color online) Log-log plot of *k* versus wavelength compared with the literature data of Soufli et al.[18], Monaco et al. [17], Blumenstock et al. [2], three interpolation ranges, the reststrahlen band obtained from Samara et al. [21], along with literature data for B [31, 32].

Fig. 4. (color online) Log-log plot of *n* versus wavelength obtained with KK analysis compared with the present ellipsometry data, and the literature data of Soufli et al.[18], Monaco et al. [17], Blumenstock et al. [2], along with literature data for B [31]. Inset: δ versus wavelength below 20 nm

Fig. 5. (color online) B_4C film bandgap obtained as the abscissa intercept of the linear extrapolation of $\sqrt{\alpha E}$ (a) and $\sqrt{\varepsilon_2 E^2}$ (b) as a function of energy.

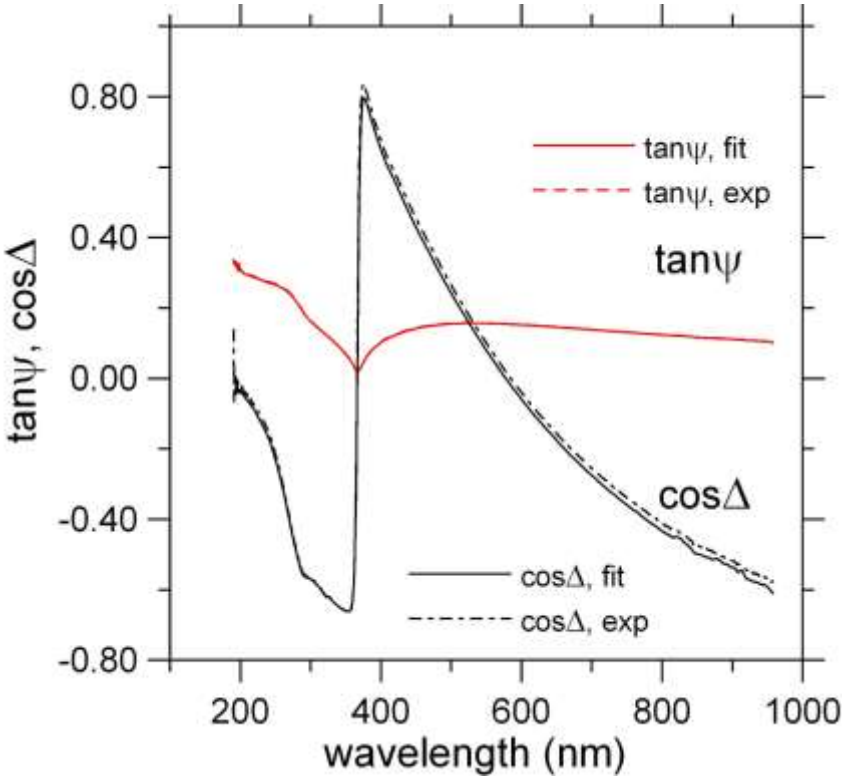
0.80
0.40
0.00
-0.40
-0.80
tanψ, cosΔ
200
400
600
800
1000
wavelength (nm)
tanψ, fit
tanψ, exp
tanψ
cosΔ
cosΔ, fit
cosΔ, exp

Fig 1

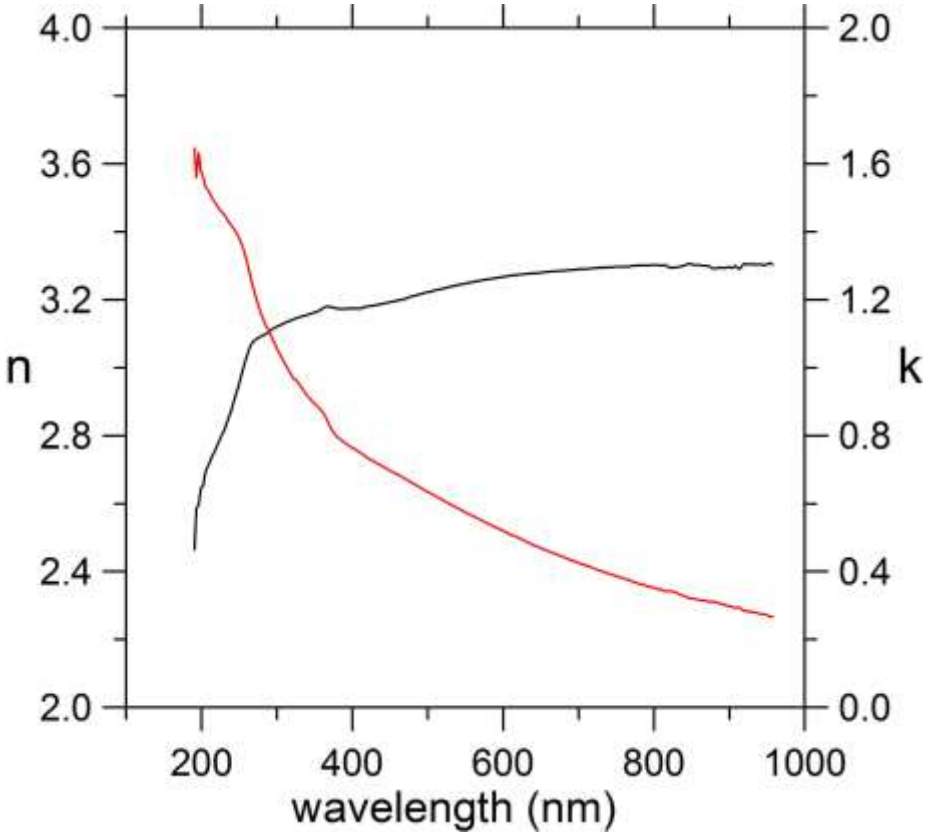
4.0
3.6
3.2
2.8
2.4
2.0
n
2.0
1.6
1.2
0.8
0.4
0.0
k
200
400
600
800
1000
wavelength (nm)

Fig 2

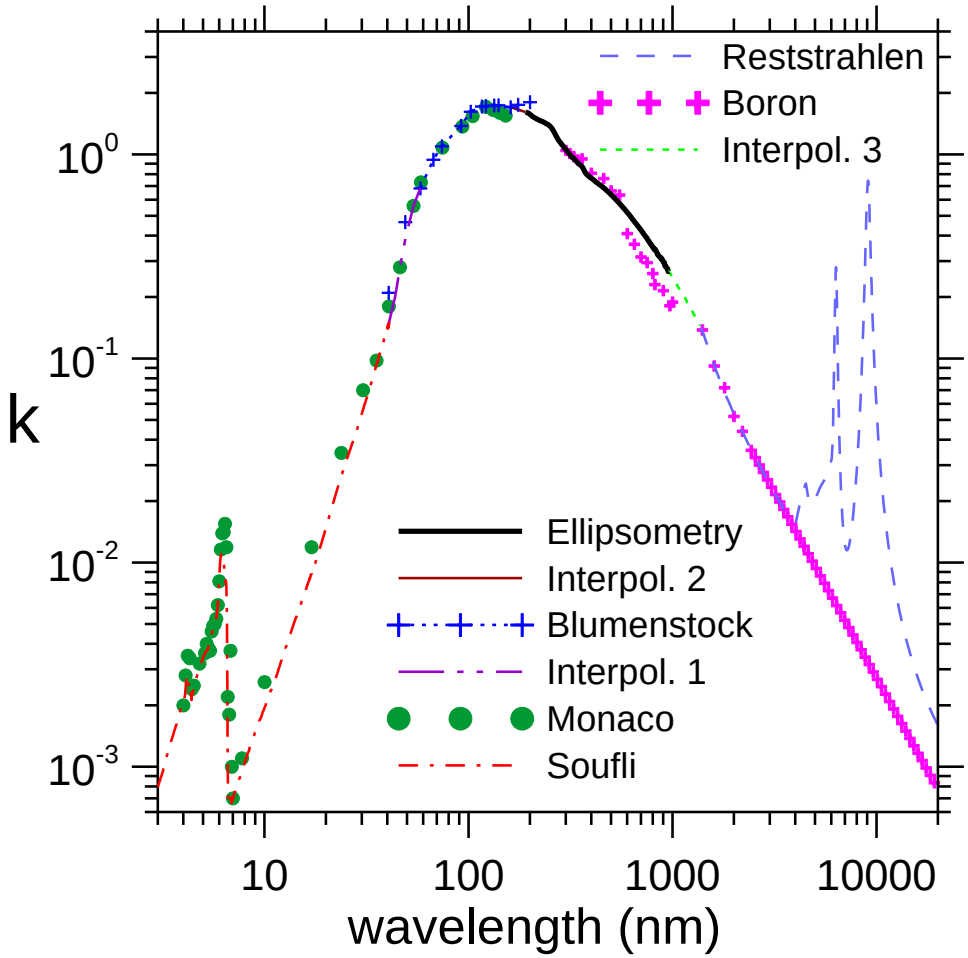
Reststrahlen
Boron
Interpol. 3
Ellipsometry
Interpol. 2
Blumenstock
Interpol. 1
Monaco
Soufli
k
10^{0}
10^{-1}
10^{-2}
10^{-3}
10
100
1000
10000
wavelength (nm)

Fig. 3

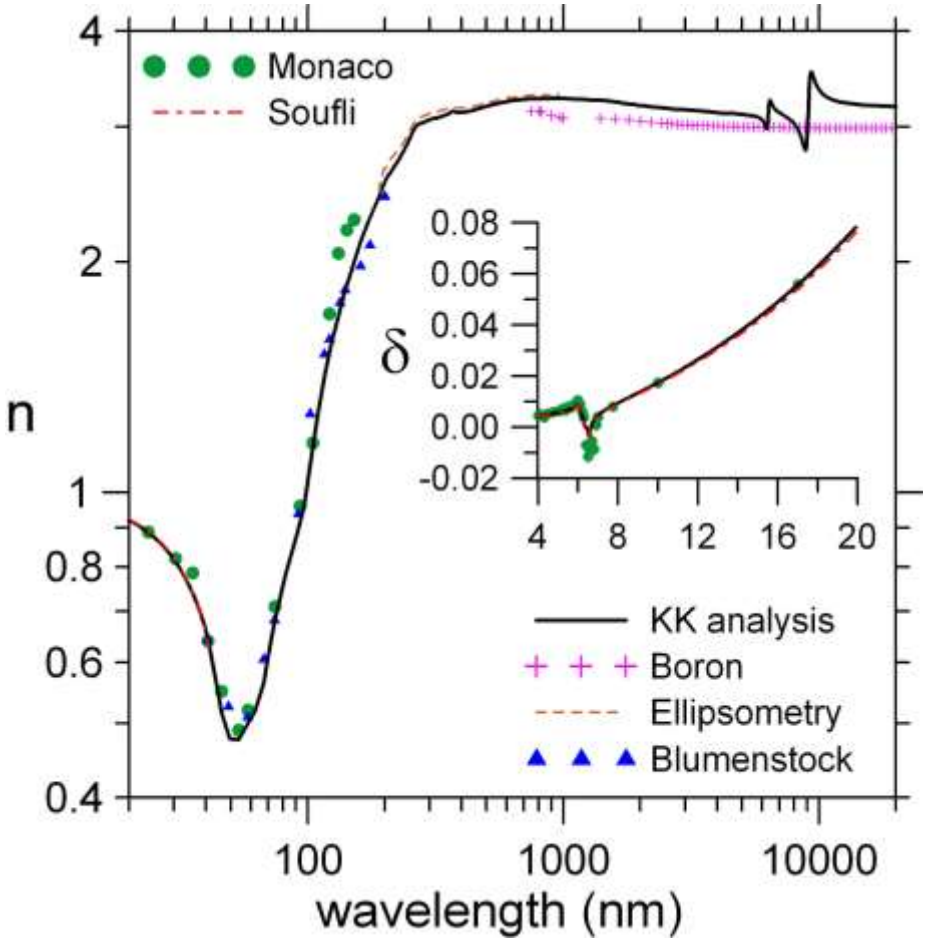
Monaco
Soufli
KK analysis
Boron
Ellipsometry
Blumenstock
n
δ
wavelength (nm)
4
2
1
0.8
0.6
0.4
100
1000
10000
0.08
0.06
0.04
0.02
0.00
-0.02
4
8
12
16
20

Fig. 4

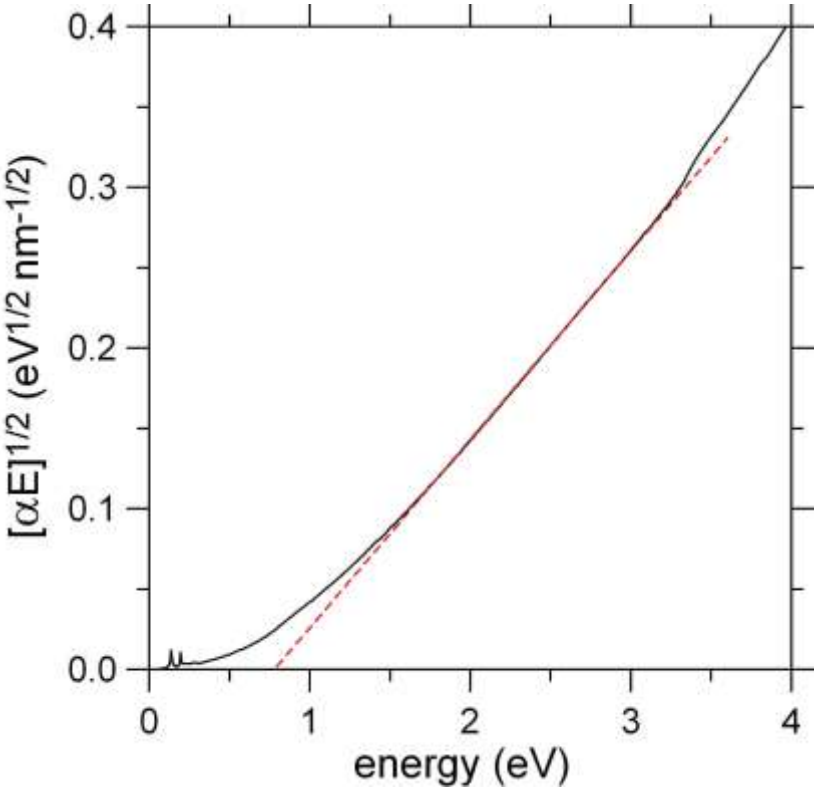

Fig 5a

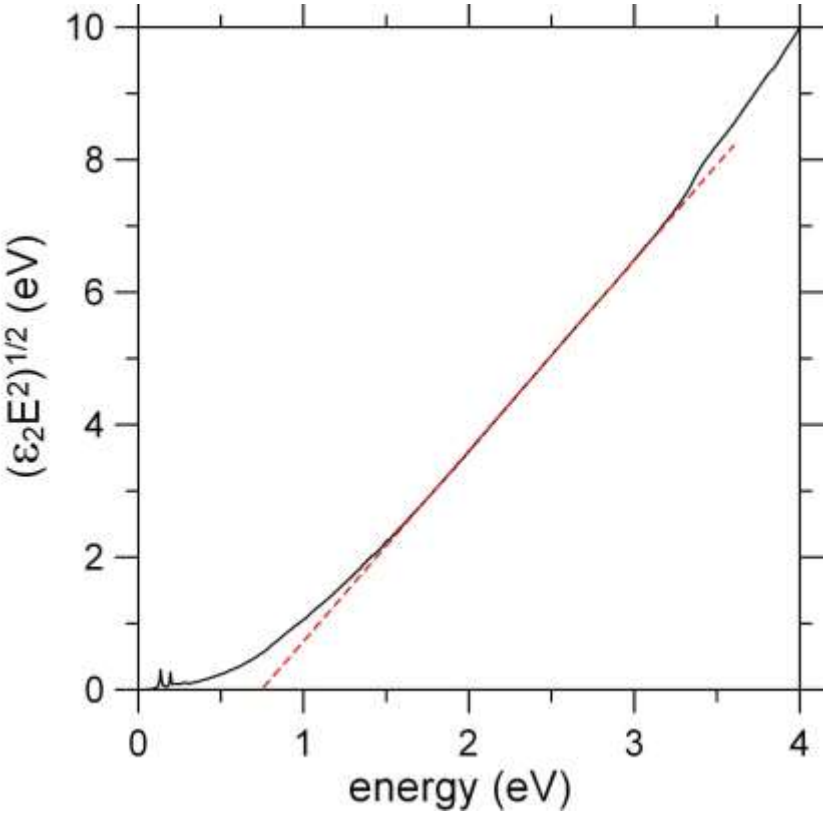

Fig. 5b